Hydrol. Earth Syst. Sci. Discuss., 10, 6359–6406, 2013
www.hydrol-earth-syst-sci-discuss.net/10/6359/2013/
doi:10.5194/hessd-10-6359-2013

Hydrology and Earth System Sciences
Open Access
Discussions

This discussion paper is/has been under review for the journal Hydrology and Earth System Sciences (HESS). Please refer to the corresponding final paper in HESS if available.

One-way coupling of an integrated assessment model and a water resources model: evaluation and implications of future changes over the US Midwest

N. Voisin[1], L. Liu[2], M. Hejazi[2], T. Tesfa[1], H. Li[1], M. Huang[1], Y. Liu[1], and R. L. Leung[1]

[1]Pacific Northwest National Laboratory, Richland, WA, USA
[2]Joint Global Change Research Institute, Pacific Northwest National Laboratory, College Park, Maryland, USA

Received: 2 April 2013 – Accepted: 26 April 2013 – Published: 22 May 2013

Correspondence to: N. Voisin (nathalie.voisin@pnnl.gov)

Published by Copernicus Publications on behalf of the European Geosciences Union.

Abstract

An integrated model is being developed to advance our understanding of the interactions between human activities, terrestrial system and water cycle, and to evaluate how system interactions will be affected by a changing climate at the regional scale. As a first step towards that goal, a global integrated assessment model including a water-demand model is coupled offline with a land surface hydrology – routing – water resources management model. In this study, a spatial and temporal disaggregation approach is developed to project the annual regional water demand simulations into a daily time step and subbasin representation. The model demonstrated reasonable ability to represent the historical flow regulation and water supply over the Midwest (Missouri, Upper Mississippi, and Ohio). Implications for future flow regulation, water supply, and supply deficit are investigated using a climate change projection with the B1 emission scenario, which affects both natural flow and water demand. Over the Midwest, changes in flow regulation are mostly driven by the change in natural flow due to the limited storage capacity over the Ohio and Upper Mississippi River basins. The changes in flow and demand have a combined effect on the Missouri summer regulated flow. The supply deficit seems to be driven by the change in flow over the region. Spatial analysis demonstrates the relationship between the supply deficit and the change in demand over urban areas not along a main river or with limited storage, and over areas upstream of groundwater dependent fields, which therefore have an overestimated surface water demand.

1 Introduction

Water is essential for a wide range of human activities including energy production and agricultural systems. Observational and modeling studies have suggested an accelerated hydrological cycle in a warmer climate (Held and Soden, 2006) and amplification of precipitation extremes (Allen and Soden, 2008). Changes in water supply can have

HESSD
10, 6359–6406, 2013

profound impacts on energy production and land use. How human systems respond to climate change can provide feedbacks on the climate and water cycle. Therefore predicting climate change requires modeling systems that represent the fully integrated natural and human components of the water cycle. This is a significant scientific challenge because the interactions underlying the coupled human–Earth system are not fully understood.

Global integrated models are being developed (Pokhrel et al., 2012; Biemans et al., 2011; Döell et al., 2009; Haddeland et al., 2006) to advance our understanding of the interactions between human activities, terrestrial system the water cycle, and how they will be affected by the changing climate at regional and global scales. In those models, water demands are represented using physically-based models, usually related to irrigation demands simulated by crop models. At regional scales, assessments of climate change impacts on water resources have been performed using integrated models of climate and hydrology, with or without water management but assuming no change in land use (e.g., National Climate Change Assessment, 2008). Recently some analyses have been performed combining the effect of land use change and climate change on natural water resources, with land use primarily driven by population and urbanization while changes in agriculture or effects of reservoir operations are not considered (Cuo et al., 2011; Mishra et al., 2010). This study represents a step towards developing an integrated model that represents both human and natural system drivers of water cycle and climate changes. The analysis presented here leverages from previous studies. We implement a subbasin configuration of a land surface model to simulate water supply (runoff and baseflow) coupled with a river routing model and a water management model, and a global integrated assessment model that simulates water demand by sector (irrigation, domestic and industrial, etc) driven by socio-economic factors, technologically detailed energy and food demands, and climate mitigation targets in a fully integrated system.

By building the links between a global integrated assessment model that provides estimates of annual water demands and a land surface scheme with river routing and a water resources model, we aim at improving the representation of the interaction pathways that govern the evolution of the hydrologic components that are integral to the energy-water and land components of the Earth system, in the context of changing climate.

The paper describes the methodology to couple the water demand component of a global integrated assessment model to the terrestrial system component consistent of a land surface model, a river routing model and a water resources management model of an Earth system model. The integrated models are driven by global simulations of current and future climate and are evaluated over the historical period using observations. Implications of combined changes in climate and human factors (socio-economics, energy and food demands, and climate mitigation targets represented by the global integrated assessment model) on future water resources are assessed from simulations by the integrated models for the future time periods. This study reports modeling and analysis over the US Midwest with strong interactions among water, energy, and land use.

The next section presents the domain and the models. Section 3 describes the approach to couple the demand model to the terrestrial system model. Section 4 evaluates the integrated model over the historical period and assesses implications for the future.

2 Domain, models and datasets

2.1 Domain

The US Midwest region is chosen for the first application of the integrated models. The domain includes the Missouri, Upper Mississippi and Ohio River basins (Fig. 1), hereinafter denoted as the Midwest Region. This region is chosen because it represents many crosscutting issues on climate, energy, land use, and water. For example,

HESSD
10, 6359–6406, 2013

the Midwest is a major area for bioenergy resource, representing potential conflicts between food and fuel.

There are 476 geo-referenced reservoirs over the region (GRanD database, Lehner et al., 2011a) and all of them are modeled in the study. Despite their small capacities, Lehner et al. (2011b) demonstrated their importance in the regulation of the flow at larger scales. Also keeping all reservoirs in the model allows us to test the model for potential applications across multiple spatial scales in the future.

Reservoir regulation for navigation is a priority in the Ohio River basin, the Upper Mississippi River basin, and along the main stem of the Missouri River. In our generic water resources model detailed below, operating rules differ for (i) irrigation only, (ii) combined irrigation and flood control, and (iii) other usages. The operating rule for other usages is consistent with navigation with the aim to have a uniform flow throughout the year. However, over the main stem of the Missouri the priority is given to irrigation, which prescribes seasonality in the monthly releases.

The Missouri has its headwater in the Rockies, which provides a late spring water storage for the agriculture rich region. The Missouri has 194 reservoirs according to the GRanD database (Lehner et al., 2011a); out of those reservoirs, 125 are used for irrigation and not flood control, 29 are used jointly for both irrigation and flood control, and the remaining 40 reservoirs are used for other uses like hydropower and supply. The Upper Missouri is used mostly for combined flood control and irrigation, the Platte River and the upper Kansas River are used for irrigation but not flood control, while the downstream Kansas and Osage Rivers are used mostly for flood control and not irrigation. The most downstream station along the Missouri River before its confluence with the Mississippi River is Hermann, MO which drains 1 371 010 km^2 of semi-arid lands.

The Ohio River lies in the eastern part of the domain and with its headwater in the Appalachians and is the main tributary in volume to the Mississippi River (Fig. 1). The Ohio River basin has 131 reservoirs after the GRanD database; none is used for irrigation, 71 are used in part for flood control. Other usages include navigation, recreation,

HESSD
10, 6359–6406, 2013

and hydropower, or water supply as this is a heavily populated region (25 million, 8 % of the US population, Ohio River Valley Sanitation Commission). The downstream station is Metropolis, IL, which drains 525 727 km^2 of humid subtropical and humid continental climate areas.

The Upper Mississippi basin has its headwaters above Minneapolis. It includes 220 reservoirs with none for irrigation and 25 for flood control. Above Minneapolis reservoirs are mostly for hydropower and recreation while downstream reservoirs are mostly for navigation; 112 of them have a reservoir capacity of less than 500 million cubic meters. The downstream station prior to the confluence with the Missouri is Grafton, IL (443 475 km^2).

2.2 Models and datasets

Figure 2 presents the schematic of the modeling approach. A water resources management model (Voisin et al., 2013) has been developed and coupled to a routing model called Model for Scale Adaptive River Transport (MOSART) (Li et al., 2013a). The coupled model, MOSART-WM, takes as input the daily runoff and baseflow generated by a land surface hydrology model, a subbasin implementation of the Community Land Model (SCLM) (Lawrence et al., 2011; Li et al., 2011), and the total consumptive water demand provided by a water demand model of the Global Change Assessment Model (GCAM) (Wise et al., 2009; Kim et al., 2006; Clarke et al., 2007a,b; Brenkert et al., 2003). The land surface scheme SCLM is forced by meteorological data statistically downscaled from global climate simulations for the historical and future periods (Fig. 2). The next sections present details about the different models.

2.2.1 A subbasin-based framework for land surface hydrologic modeling

In this study, we applied the subbasin-based version of Community Land Model version 4 (hereinafter denoted as SCLM, Li et al., 2013b), for hydrologic simulations over the study region. CLM is the land component within the Community Earth System Model

(CESM) (formerly known as Community Climate System Model – CCSM) (Lawrence et al., 2011). CLM is also the land surface component in a regional earth system model based on the Weather Research and Forecasting (WRF) model (Ke et al., 2012; Kraucunas et al., 2013; Leung et al., 2006). The capability of CLM4 for hydrologic simulations has recently been assessed at small watershed to larger basin scales (Huang et al., 2013; Li et al., 2011, 2013b). In the subbasin-based framework (Li et al., 2013b), land surface hydrologic processes such as water and energy transfer between the land surface and the atmosphere, as well runoff generation, are represented by treating each subbasin as a pseudo grid cell without significantly modifying the existing CLM modeling structure. Subbasin boundaries within the study domain were delineated using ArcSWAT (Neitsch et al., 2005). The study area was delineated into 18 681 subbasins with $\sim 120\,\mathrm{km}^2$ average size. Soil, vegetation and land cover characteristics of each subbasin in the study domain were derived from the 0.05° CLM4 input dataset developed by Ke et al. (2012), by overlaying the watershed boundaries with the data layers and aggregating to each basin using an area weighted average algorithm following Li et al. (2013b). Hydrologic parameters relevant to topography were obtained by processing the 90 m resolution DEMs from HydroSHEDS (Lehner et al., 2011a), consistent with the SCLM model setup in Li et al. (2011, 2013b) and Huang et al. (2013). SCLM was spun up using hourly forcing described below for the historical period 1976–1999 for 10 cycles (300 yr total) until all the state variables reached equilibrium.

2.2.2 Atmospheric forcing data

Daily precipitation and temperature at 1/8 degree resolution were retrieved from the Computational Assessments of Scenarios of Change for the Delta Ecosystem (CASCaDE) dataset (http://cascade.wr.usgs.gov). The CASCaDE dataset was developed by applying the constructed analog statistical downscaling method (Hidalgo et al., 2008) to the historical and future climate simulations generated by Geophysical Fluid Dynamics Laboratory Coupled Climate Model (GFDL CM2.1) (Delworth et al., 2006) for the Coupled Model Intercomparison Project (CMIP3). The future climate simulation followed the Special Report for Emission Scenarios SRES B1 emission scenario. The downscaled daily precipitation and temperature time series from 1975–2100 were processed using forcing disaggregator of the Variable Infiltration Capacity (VIC) (Liang et al., 1994) (http://www.hydro.washington.edu/Lettenmaier/Models/VIC/Documentation/VICDisagg.shtml) to generate hourly precipitation, temperature, shortwave radiative fluxes using the MTCLIM 4.2 algorithm (Thornton and Running, 1999; and Thornton et al., 2000), incoming longwave radiating fluxes (the Tennessee Valley Authority algorithm, TVA, 1972), specific humidity (Kimball et al., 1997) required by SCLM. Wind speed and surface pressure data were obtained from the North American Land Data Assimilation System (NLDAS) (Mitchell et al., 2004). The data were then projected to the subbasin boundaries discussed earlier using an area average algorithm as inputs into SCLM. The GFDL-B1 climate scenario portrays the B1 emissions scenario (representing a future where greenhouse gas emissions are curtailed by mid-century) as modeled by the medium-sensitivity GFDL CM2.1 model. It represents a middle-of-the-road future climate among the multiple global circulation model and greenhouse gas emission scenarios.

2.2.3 The water resources management model (MOSART-WM)

The water resources model (WM, Voisin et al., 2013) relies on generic operating rules adjusted independently for each reservoir; monthly release targets are based on the long term mean monthly inflow, the long term mean monthly demand associated to each reservoir, and reservoir characteristics (storage and uses). Initial work by Hanasaki et al. (2006) and Biemans et al. (2011) included two types of rules in particular: (i) monthly varying releases based on water demand, hydroclimatic characteristics and storage capacity for reservoirs used for irrigation, or (ii) for all other uses release of mean annual flow adjusted for monthly demand anomalies (flood control, navigation, conservation, recreation). Voisin et al. (2013) updated the release targets and complemented them with storage targets in order to improve joint flood control and irrigation uses. The WM includes: (i) a local extraction module that extracts from the local surface water and river channel to provide in priority for the local demand, (ii) a reservoir module that simulates the reservoir storage, regulates the releases and provide supply to each grid cell in need, (iii) an inter-dependency database that allows managing the request of water to reservoirs and the distribution of supply to grid cells. The seasonal patterns of the operating rules is monthly, and there is inter-annual variability of those monthly pre-set releases based on the initial storage at the start of the irrigation season. However the extraction is performed at the time step of the run – presently daily. Releases adjustment for spilling, minimum environmental flow and drying reservoirs are also made at the time step of the run. The WM is coupled to the Model for Scale Adaptive River Routing (MOSART) (Li et al., 2013a) river routing model. In this experiment, MOSART-WM is run independently of the land surface model (SCLM) described above. As such, return flow is not explicitly simulated. Input for MOSART-WM includes daily surface and sub-surface runoff, and daily total water consumptive demand, not withdrawals, provided by the water demand model described below. However, an estimate of withdrawals is used for the optimal calibration of the release targets as explained in Voisin et al. (2013).

2.2.4 GCAM

The global change assessment model (GCAM) is a dynamic-recursive model that encompasses technologically-detailed representations of human and natural systems and their interactions (Wise et al., 2009; Kim et al., 2006; Clarke et al., 2007a,b; Brenkert et al., 2003). The model includes representations of global economy, the energy system, agriculture and land use, and climate. It models global trade in fossil energy and agricultural products and solves for prices of all energy, agricultural, and forest productivities to balance off demands and supplies (Calvin et al., 2013). This is useful, even though the focus of the work is regional in nature (e.g., Midwest), because global decisions associated with adhering to the adopted B1 climate mitigation scenario has regional implications (e.g., bioenergy production in the Midwest Region).

HESSD
10, 6359–6406, 2013

Recently, Hejazi et al. (2013a,b) explicitly incorporated sectoral water demand modules in GCAM to estimate the amount of freshwater demanded on an annual basis. The water demand modules account for the annual amount of water demanded by a set of individual sectors, namely: irrigation (Chaturvedi et al., 2013), electricity generation (Davies et al., 2013; Kyle et al., 2013), livestock, domestic purposes (Hejazi et al., 2013c), primary energy production, and manufacturing (Hejazi et al., 2013a). GCAM tracks water withdrawals and consumptive use by region (14 geopolitical regions or 151 agro-ecological zones – Monfreda et al., 2009), by sector (e.g., irrigation, electricity, etc.) and subsectors (e.g., fuel type, crop type, etc.), and technology (e.g., cooling technologies: once-through, recirculating, cooling ponds, and dry cooling). That information is passed on to the water resources model as the demanded amount of consumptive water use by sector. Note, GCAM's water demand estimates are not constrained by the amount of water availability in a basin. When considering river and reservoir routing and human activities within the runoff generation modeling framework plus the seasonality of water availability and existing reservoir storage capacity, not to mention the modeling uncertainties, the suggested demand by GCAM might end up being infeasible when integrated with SCLM/MOSART/WM. In this research, we track the amount of supply deficit (i.e., unmet consumptive water demands). More details about the water demand methodology in GCAM can be found in Hejazi et al. (2013a).

3 Coupling of the water demand and water management models

A one-way coupling between GCAM and SCLM-MOSART-WM is the focus of this paper. There is, however, a mismatch in scale both spatially and temporally among the models. GCAM is solved on a 5 yr time step and operates at the regional scale (14 geopolitical regions & 151 AEZs) which are much coarser than what would be required by SCLM-MOSART-WM. The temporal and spatial disaggregations to the subbasin and daily resolution of MOSART-WM need to represent spatio-temporal variations of use over the basin. This has implications to the locally available water supply and affects

HESSD
10, 6359–6406, 2013

the WM as operating rules of each reservoir are a function of the monthly climatology and magnitude of the demand associated to each reservoir. Disaggregation affects the distribution of water supply to the different grid cells. Thus, to facilitate the proposed coupling, both spatial and temporal downscaling steps were employed as described next.

3.1 Spatial downscaling

We adopted the downscaling methodology of Hejazi et al. (2013a) to downscale the individual sectoral demands (irrigation, livestock, municipal, electricity generation, primary energy, and manufacturing water demands) from regional scale (AEZ and GCAM regional scale) to the grid scale ($0.5^{\circ} \times 0.5^{\circ}$), and subsequently to the subbasin scale. In a nutshell, the downscaling algorithms employ proxy information such as population and areas equipped with irrigation information to map water demands to a finer spatial scale of 0.5°. To assess the accuracy of GCAM in combination with the downscaling algorithms in estimating water demands at the regional scale, the spatially downscaled annual sectoral water demands from GCAM are compared against the state-level USGS inventory for the years of 1990 and 2005. The six sectors of water demand are assorted into irrigation and non-irrigation (electricity + domestic + mining + livestock + manufacturing) water demands for the purpose of simplification. The total water withdrawals and consumptive use produced by GCAM show a good agreement with USGS values on the state level (Fig. 3). The statistics of the results are shown in Table 1.

3.2 Temporal downscaling

GCAM annual water demand estimates with 5 yr increments need to be temporally disaggregated to daily for input into MOSART-WM. The disaggregation is performed in several steps, first a continuous annual time series of water demands was obtained by linearly interpolating between the 5 yr intervals. Then the annual values are downscaled

HESSD
10, 6359–6406, 2013
Integrated assessment of US Midwest water resources
N. Voisin et al.

to monthly through a suite of techniques as described below, and, finally, the monthly demand are downscaled to daily using a uniform distribution. This section presents the disaggregation to the monthly time scale. Wada et al. (2011) devised a set of simple methods to map non-irrigation sectors from annual to monthly time step. We adopted their approaches for domestic, mining, livestock and manufacturing, extended the electricity generation technique, and simplified the irrigation one. Each of the steps is described next with validation results.

3.2.1 Irrigation

Unlike the work of Wada et al. (2011) who used a crop growth model to estimate monthly irrigation water requirements, crop water requirements in GCAM are computed using a simplified methodology that utilizes estimated coefficients of water requirement per crop type and AEZ from crop growth models to efficiently compute irrigation water on an annual basis (see Chaturvedi et al., 2013). This reduced form is essential to the computational feasibility of iterating food demands and prices hundreds of iterations in each GCAM time period without resorting to running a crop growth model that many times. Chaturvedi et al. (2013) provide a detailed comparison to other literature estimates and statistics at the regional scale. Figure 3 shows a comparison of the estimated total irrigation against USGS estimates for water withdrawals at the state level in year 2005. The next step is to temporally downscale GCAM results of irrigation water demand to monthly time series.

The monthly profile for downscaling GCAM irrigation water demand from annual to monthly was obtained from Siebert and Döll (2008) by using irrigation results from the Global Crop Water Model (GCWM). GCWM provided global gridded monthly irrigation water requirements for 26 crop types, which were mapped to the twelve GCAM crop categories to estimate the crop and region specific monthly distribution of irrigation. This enabled us to construct irrigation water use monthly profiles for each of the AEZ regions in the US (Fig. 4a). Following the work of Hanasaki et al. (2012a,b), we applied the same monthly profile for irrigation water withdrawal and consumption. Therefore,

HESSD
10, 6359–6406, 2013

irrigation water withdrawal and consumption from GCAM were downscaled from annual to monthly time step by applying the ratios calculated from the monthly profiles distinguished by AEZ (Eq. 1).

$$W_i = W_a \times \mathrm{Ratio}_{\mathrm{AEZ}} \quad (1)$$

where W_i indicates irrigation water demand for the month of i, and W_a indicates annual irrigation water demand.

3.2.2 Electricity

In this study, the temporal downscaling of electricity water demands in the US was built on the basis of electricity use fluctuations within a year. We assume that the amount of water used for generating electricity in a particular month is proportional to the amount of electricity generated in each month. In GCAM, electricity generation is consumed by three main sectors: industry, transportation, and building. Industry and transportation sectors are assumed to consume equal shares of electricity within a year (i.e., uniform distributions). A simple algorithm is developed to reflect the seasonal fluctuations of electricity use in the building sector based on the concepts of Heating Degree Days (HDD) and Cooling Degree Days (CDD). HDD and CDD are measurements designed to reflect the demand for energy needed to heat/cool a building. It is derived from measurements of outside air temperature.

About 20 % of the total electricity used in buildings in the US is used for heating (5 %) and cooling (15 %) purposes the remaining 80 % is used by other home utilities. These values are taken directly from GCAM. In this study, only the heating and cooling electricity shares are assumed sensitive to the climate signal. Equation (2) describes

HESSD
10, 6359–6406, 2013

the downscaling methodology of annual building electricity use to monthly scale.

$$E_{\mathrm{bi}} = E_{\mathrm{ba}} \times \left(0.05 \frac{\mathrm{HDD}_i}{\sum_1^{12} \mathrm{HDD}_i} + 0.15 \frac{\mathrm{CDD}_i}{\sum_1^{12} \mathrm{CDD}_i} + 0.8 \times \frac{1}{12} \right) \tag{2}$$

where E_{bi} indicates electricity used by building sector for the month of i, E_{ba} indicates annual electricity used by building sector, HDD is for heating degree days (Eq. 3) and CDD is for cooling degree days (Eq. 4) in month i:

$$\mathrm{HDD}_i = \sum_d^n (18 - T_d)\ \forall T_d < 18° \tag{3}$$

$$\mathrm{CDD}_i = \sum_d^n (T_d - 18)\ \forall T_d > 18° \tag{4}$$

where T_d is the mean daily temperature in day d. Since building sectors consume 74 % of the total electricity generated and other sectors (industry and transportation) consume 26 %, the final algorithm for the monthly downscaling is

$$E_i = E_{\mathrm{a}} \times \left(0.74 \times \left(0.05 \frac{\mathrm{HDD}_i}{\sum_1^{12} \mathrm{HDD}_i} + 0.15 \frac{\mathrm{CDD}_i}{\sum_1^{12} \mathrm{CDD}_i} + 0.8 \times \frac{1}{12} \right) + 0.26 \times \frac{1}{12} \right) \tag{5}$$

HESSD
10, 6359–6406, 2013

where E_i indicates electricity used in month i, and E_a indicates annual electricity used. The monthly water demand for electricity generation, therefore, is

$$W_i = W_a \times \left(0.74 \times \left(0.05 \frac{\mathrm{HDD}_i}{\sum_1^{12} \mathrm{HDD}_i} + 0.15 \frac{\mathrm{CDD}_i}{\sum_1^{12} \mathrm{CDD}_i} + 0.8 \times \frac{1}{12} \right) + 0.26 \times \frac{1}{12} \right) \tag{6}$$

where W_i indicates total thermoelectric water demand in month i, and W_a indicates annual thermoelectric water demand. As shown in Fig. 4b, the total water withdrawal for electricity generation are downscaled to monthly level (using Eq. 6) and compared to the total electricity generation in year 2005. HDD and CDD are calculated from bias corrected and downscaled GFDL temperature historical and future simulations.

3.2.3 Domestic

Domestic water demand is temporally downscaled using the algorithm developed by Wada et al. (2011). The equation is

$$W_i = \frac{W_a}{12} \left[\left(\frac{T - T_{avg}}{T_{max} - T_{min}} R \right) + 1.0 \right] \tag{7}$$

where W is water demand, "a" stands for annual, i stands for monthly, T is monthly temperature, T_{avg}, T_{min}, T_{max} are average, minimum and maximum temperature over the year, R is an amplitude (dimensionless), which adjusts the relative difference in domestic water demand between the months with the warmest and the coldest temperatures.

Wada et al. (2011) suggested an R of 0.1 based on their assessment in Spain and Japan. However, this term is found to be closer to around 1.0 in the US based on four cities that lie within four climate zones (see Fig. 4c).

HESSD
10, 6359–6406, 2013

3.2.4 Mining, livestock and manufacturing

For the temporal downscaling of water demand in mining, livestock, and manufacturing sectors, a uniform distribution (1/12) is applied following the work of Wada et al. (2011).

The historical monthly downscaled sectoral water demand results are shown in Fig. 5, divided into four categories: irrigation consumption, irrigation withdrawal, non-irrigation consumption and non-irrigation withdrawal. Figure 5a, b shows the total annual water demands for the Midwest region, and the monthly time series after applying the temporal downscaling step, respectively. By spatially downscaling demands, a similar time series is generated for each of the subbasins. Water demands in summer are relatively higher than in winter for both irrigation and non-irrigation sectors. Future water demands are derived similarly using bias corrected and downscaled GFDL temperatures data.

4 Evaluation and future implications

We first evaluate the simulated impact of anthropogenic activities on the simulated historical flow (1984–1999) at the outlet of the three regions of interest: Missouri, Upper Mississippi, and Ohio. The impact on flow and the supply deficit as simulated by historical GCAM-SCLM-MOSART-WM are both analyzed with respect to the baseline SCLM-MOSART simulated natural flow. Future water resources, i.e. future regulated flow and water supply, are affected by changes in natural flow and in water demands. Operating rules based on historical flow are kept unchanged throughout the future simulation for that purpose (see discussion section). To evaluate the implications of predicted anthropogenic activities on the projected water resources of the Midwest, we compare the predicted change in natural flow (climate change effect only) and the predicted change in regulated flow (combined climate and demand changes). We isolate the main drivers for the predicted change in water supply: changes in flow and/or demand by regions, which differ in their type of demands, storage capacity, and operating rules (Fig. 1).

HESSD
10, 6359–6406, 2013

4.1 Historical evaluation

Over the 1984–1999 period, we evaluate the change in flow due to the human activities including regulation and extraction of water over the three regions. We also evaluate the water supply deficit. Spun-up SCLM forced with historical statistically downscaled GFDL meteorological forcing provides the daily surface runoff and baseflow forcing. The routing model MOSART is run in a first step in order to simulate the naturalized flow at the three locations of interest, the baseline scenario. It also provides the long-term mean monthly flow used to update the operating rules. GCAM provides the daily total water consumptive demand to the water resources model MOSART-WM to simulate the regulated flow and water supply.

Figure 6 shows the mean monthly simulated and observed natural and regulated flow over the three regions, and the relative change in flow due to anthropogenic influence for the historical period only. Figure 7 shows the simulated long-term annual time series of natural and regulated flows at the same locations. Only at Hermann are both the naturalized and regulated flow available. At Metropolis and Grafton, the regulation at the monthly time scale is deemed negligible given the storage capacity over the basin. The downscaled GFDL climate tends to be drier with higher radiative forcing then the forcing from the North American Land Data Assimilation System (NLDAS2) (Cosgrove et al., 2006), which is derived from observed temperature and precipitation data. The biases in the atmospheric forcing lead to an overall underestimation of runoff. The runoff coefficients over the different regions using either the downscaled GFDL or NLDAS as forcing to SCLM are both around 0.17, 0.32, and 0.39 at Hermann, Grafton and Metropolis, respectively. As a reference the Maurer et al. (2002) hydrological simulations using the calibrated Variable Infiltration Capacity (VIC) hydrology model (Liang et al., 1994) and station based meteorological forcing have runoff coefficients of 0.16, 0.21, and 0.40 at the same locations although their simulated flow is more in agreement with observations. See the discussion section for more details on the uncertainty in the hydrologic simulations. The right column in Fig. 6 shows the monthly impact of

HESSD
10, 6359–6406, 2013

extraction and regulation on the naturalized flow. Table 2 shows the annual effect of river regulation and extraction on the natural flow. Both over the Ohio and the Upper Mississippi the extraction and regulation are minimal at the monthly and annual time scales (−0.8 and −6.6 % respectively), in agreement with observations. Over the Missouri, the regulation drives to a 24 % loss in the annual discharge. The seasonal effect of extraction and regulation on the natural flow is in agreement with observations but over the October–December low flow period, the change tends to be of opposite sign. Given the simplified generic operating rules, the human activities on the flow are reasonably well-captured by the SCLM-MOSART-WM integrated model forced with GCAM demand and the downscaled GFDL historical climate.

Figure 8 shows the regional average monthly demands and supply deficit for the historical period and Table 3 shows the historical relative annual water supply deficit. Over the Midwest the supply deficit is around 3 % which is consistent with the "rain-fed" crop region characteristics especially on the Missouri (1.5 % deficit only). As discussed later, the supply deficit is localized in the southwest Missouri basin where deep groundwater pumping is used and over the urban areas around the Great Lakes, which can also be used as additional freshwater source.

4.2 Future implications

4.2.1 Demand and natural flows

Figure 8 shows the GCAM mean monthly total water demand for the historical period, 2030s, 2050s and 2080s for the Missouri, Upper Mississippi, Ohio and the entire Upper Midwest. The increase in total water demand keeps increasing over the entire future period over the Missouri, up to 60 % over the irrigation season. GCAM projects the total demand to significantly increase by the 2030s with a slower increase thereafter to the 2050s and then to stagnate by the 2080s over the Ohio and Upper Mississippi only. The Upper Mississippi and Ohio have the largest relative increase in demand during summer time, up to 75 % even though it stabilizes after 2050 (Fig. 9).

HESSD
10, 6359–6406, 2013

GCAM projects the consumptive irrigation demand to keep increasing over the Midwest while the non-irrigation consumptive demand increased at a very slow and approximately constant rate (Fig. 5). With the fraction of irrigation demand over the total demand decreasing over the Ohio and Upper Mississippi in the future (Table 3), the demand plateau over the two regions is associated with domestic and thermoelectric demands based on a population projected to stagnate by 2050 in the B1 scenario.

We force SCLM-MOSART with the downscaled GFDL B1 future meteorological forcing. Figure 10 shows the predicted naturalized flow due to climate change over the three regions. Figure 10 also shows the relative change of natural flow with respect to the historical simulations. The region is predicted to have a warmer climate and overall more precipitation, leading to an overall increased annual natural flow, and higher snowmelt while summer flows decrease (Fig. 10). The increased annual flow, higher snowmelt and lower summer flow tend to be similar between the 2030s and 2050s but further accentuate by the 2080s. The effects of climate change on natural flow over the Midwest are consistent with the findings of others (Mishra et al., 2010; CCSP 2008).

We further force SCLM-MOSART-WM with the downscaled GFDL B1 future meteorological forcing with GCAM demand corresponding to the downscaled GFDL B1 scenario emission climate.

4.2.2 Flow regulation

Figure 10 shows the projected mean monthly regulated flow for future period and the relative change in regulated flow with respect to the historical regulated flows. The change in operations is not taken into account as operating rules are calibrated using the historical demands and flows (see discussion). The relative change in monthly regulated flow (solid line) due to changes in climate (GFDL-B1) and demand (GCAM) is projected to be very close to the relative change in natural flow (dashed) due to climate change only over the Ohio and Upper Mississippi basins; the change in regulated flow over those regions is driven by the change in natural flow. Over the Missouri in July, August and September, starting in the 2050s, the change in regulated flow (climate and

HESSD
10, 6359–6406, 2013

demand) is twice the magnitude, or same magnitude but of opposite sign, compared to the change in naturalized flow. The summer Missouri regulated flow is impacted as much by the change in natural flow as by the change in demand. Note that GCAM demand is not constrained by water availability.

4.2.3 Supply

Figure 8 shows the projected mean monthly water supply deficit over the Missouri, Upper Mississippi, Ohio, and Upper Midwest. Figure 9 shows the change in relative water supply deficit, which characterizes the need for and the reliance on an additional source of water supply in the future. The supply deficit is expected to keep increasing over the Missouri, stagnate over the Ohio by the 2050s, and slow in its increase in the Upper Mississippi (Table 4). The largest demand being over the Missouri, the supply deficit over the entire Upper Midwest follows its increasing trend. The end of the summer is the most vulnerable period. In terms of relative supply deficit and dependence on other source of supply, the Missouri is projected to experience its dependence jump from below 5 % to up to 15 % by 2080s for the month of September. The Missouri has the largest increase in annual relative supply deficit from 1.5 % for the historical period to 9 % by the 2080s but the Upper Mississippi has the largest dependencies; 9 % historically to 13 % by the 2080s (Table 3).

Figure 11 displays the spatial distribution of the GCAM annual consumptive water demand, the simulated SCLM-MOSART-WM water supply, and the corresponding relative supply deficit for the historical and future periods. The GCAM demands are projected to increase in particular over the Platte River and urban area over the Ohio and Upper Mississippi river basins. The supply increases where the demand increases. However, the supply deficit does not obviously overlay the regions with the highest demand, but rather seems to be a combination of demand and water availability, i.e. upstream of the Osage River and the urban areas adjacent to the Great Lakes.

HESSD
10, 6359–6406, 2013

5 Discussion

In view of the results and methodology, we highlight three areas of discussion: (i) the sensitivity of the integrated modeling results with respect to hydrologic and other modeling errors, (ii) drivers of change in projected stream discharge and ability to meet the water demand (iii) reconciliation of SCLM and GCAM water balances through the input of withdrawals in addition to consumptive demand, groundwater supply, and full coupling between WM and SCLM and water allocation when demands exceed water availability.

5.1 Modeling errors

The SCLM-MOSART simulations driven by the downscaled GFDL historical climate produced an overall underestimation of the observed naturalized flow, at Hermann. Table 5 shows the regional water balance of the GFDL-SCLM-MOSART simulations compared to the SCLM-MOSART simulations driven by the NLDAS2 forcing data. The downscaled GFDL climate is drier and has higher net radiation compared to NLDAS2, with the differences larger in 1984–1999 than 1976–1999. This results in lower runoff in GFDL-SCLM-MOSART than NLDAS-SCLM-MOSART. The bias in the downscaled GFDL climate is not surprising, as very little constraints are used in global climate simulations. Even statistical downscaling methods such as the constructed analog cannot fully remove the biases in the climate simulations. Using an ensemble of climate models may reduce overall biases, but this is beyond of the scope of this study. The runoff coefficients, however, are similar to those extracted from the Maurer et al. (2002)'s simulations, which are often used as reference. Despite simulation biases, the numerical experiments report here showed a proof of concept in one-way coupling of a terrestrial system model that includes a land surface model, river routing model and water resources management with a water demand model, which is part of a global integrated assessment model. Our results showed reasonable agreement in simulating the effect of human activities on the land surface system.

The present results focus on projection of water resources based on historical operating rules, that is, no adaptation of reservoir operations to climate change. Previous studies have applied water resources management models under climate change regionally (Hamlet et al., 2010; Christensen et al., 2004; Van Rheenen et al., 2004; Vano et al., 2011a,b) using optimized water resources operations with the full knowledge of future flow. Konar et al. (2013) applied for a first time a future scenario on crop productivity using the Hanasaki et al. (2008) global reservoir model with generic operating rules based on historical conditions as well. Quantifying the sensitivity of updating the operating rules to future flow and demand is a subject for more research. We anticipate that updating the operating rules for flow over a dependent period, i.e., equivalent to optimization, could affect the supply deficit results in this research. Sensitivity should be a function of changes in monthly natural flow and storage capacity over the region and reservoir uses.

5.2 Drivers of change in future human effects on land surface system

We investigate the drivers of the change in regulated flow and supply deficit. Figure 12 presents scatterplots of annual change in regulated discharge and annual relative change in supply deficit. Over the Ohio River basin, the demand is localized over specific urban areas (Fig. 11) and exceeds the locally available water. Cities might be located too far from the main stem from which they could request water from reservoir releases. Mostly, the reservoir storage along the main stem does not allow much regulation at the monthly time scale (Figs. 1, 6 and 7). Because of the storage capacity of the reservoirs over the Ohio River, climate change effects on the natural flow drive the change in regulated flow (Fig. 9). Changes in supply deficit are driven by a combination of changes in demand and runoff (Fig. 12).

Over the Upper Mississippi, the increase in demand with increasing supply deficit is localized over the urban and agricultural areas adjacent to the Great Lakes. There are cities like St. Louis along the main stem that actually have very small, see no supply deficit (Fig. 11). According to Fig. 12, the supply deficit is driven by the change in runoff.

HESSD
10, 6359–6406, 2013

Over the Missouri river basin, the increase in demand is spread out with a large demand along the Platte River valley. However, the supply deficit is mostly localized over the headwaters of the Platte River. As seen in Voisin et al. (2013), an excessive surface water demand can drive upstream reservoir dry leaving headwater areas with a supply deficit. The area is relying significantly on groundwater pumping (Kenny et al., 2005). Voisin et al. (2013) recommend to adjust the withdrawals and consumptive use demand on the surface water system for groundwater. The sensitivity to the fraction of irrigation groundwater use is the focus of further research. With regulated runoff being affected by a combination of change in natural flow and in demand (Fig. 9), Fig. 12 links the change in supply deficit to the change in regulated runoff, i.e. changes in natural flow and demand.

5.3 Water balance

GCAM uses an independent model to simulate water balance than SCLM, and, thus, GCAM's estimates of water demands may be inconsistent with the water availability in SCLM. This can be resolved once a two-way (full) coupling between is GCAM and SCLM-MOSART-WM is established, where the latter provides the amount of water availability and thus constraining water demands in GCAM (Tamea et al., 2013; Konar et al., 2013). We need to quantify how much groundwater comes from unconfined aquifer and how much comes from return flow for adjusting the demand on the surface water system. Similarly, in order to use withdrawals more research focused on the full coupling of the water resources management model with the land surface hydrology model is needed.

6 Conclusions

"Socio-hydrology" is a new science that fosters the understanding of human influence (flood control, agriculture, navigation, energy, and global trades) on the earth system

HESSD
10, 6359–6406, 2013

(Sivapalan et al., 2012). In this paper, a temporal downscaling methodology is developed in order to facilitate the coupling of a global integrated assessment model with a land surface scheme – routing – water resources management model. The evaluation of the integrated system is performed over three regions of the Upper Midwest: Missouri, Upper Mississippi and Ohio River basins focusing on the change from natural to regulated flows and demand and fractional supply deficit.

1. Over the historical period, the integrated system is reasonably well reproducing the anthropogenic influence on the flow and the water supply over the three regions.

2. Implications for future water resources affected by the human influence are driven by changes in the water demands simulated by GCAM and the change in flow (climate change). With the Upper Midwest projected (GFDL-B1) to have an increased in annual flow and in particular snowmelt flows:

   a. The regulated flow is projected to increase over the snowmelt period and remain similar to historical regulated flow during the summer.

   b. The supply is also projected to increase but not enough to compensate the increase in demand. The relative supply deficit is projected to increase over the region. The largest relative supply deficit is simulated over the Upper Mississippi.

   c. Drivers of the changes in regulated flow are the changes in the natural flow due to climate change for the Ohio and Upper Mississippi, and a combination of changes in socio-economic and natural flow over the Missouri.

   d. Drivers of the change in supply deficit are the changes in natural flow over the Midwest in general, Upper Mississippi. The change in supply deficit over the Ohio is driven by the change in demand that is very localized around urban areas. The change in supply deficit over the Missouri is driven by a combination of change on demand and in natural flow.

HESSD
10, 6359–6406, 2013

Over the Midwest where the flow is projected to increase and the crop is mostly rain fed, changes in regulated flow and supply, and supply deficit are driven by the change in runoff due to climate change, more than the change in socio-economic water demands. Regionally however the modeling of water demands allows us to isolate sectors and areas that will be more sensitive to change in demand and will rely on groundwater and virtual water trade. Over areas relying more heavily on irrigation, we anticipate a stronger signal between the change in demand and change in supply deficit and flow regulation. Future work will focus on the effect of hydrologic errors and on updating the reservoir module operating rules over more regions.

Acknowledgements. The authors would also like to thank Stephan Siebert at the University of Bonn, Germany for providing the global gridded monthly irrigation water requirements data for crops, and Duane Ward at the Pacific Northwest National Laboratory (PNNL) for his assistance with the WM dependence database set up over the Midwest. This study was supported by PNNL's Platform for Regional Integrated Modeling and Analysis (PRIMA). The authors wish to express appreciation to the Integrated Assessment Research Program in the Office of Science of the US Department of Energy (DOE) for long-term support that enabled the development of the Global Change Assessment Model, which was used in the conduct of this research. PNNL is operated by Battelle for the US DOE under contract DE-AC05-76RL01830. The views and opinions expressed in this paper are those of the authors alone.

References

Allen, R. P. and Soden, B. J.: Atmospheric warming and the amplification of precipitation extremes, Science, 321, 1481–1484, doi:10.1126/science.1160787, 2008.

Backlund, P., Janetos, A., Schimel, D., Hatfield, J., Boote, K., Fay, P., Hahn, L., Izaurralde, C., Kimball, B. A., Mader, T., Morgan, J., Ort, D., Polley, W., Thomson, A., Wolfe, D., Ryan, M., Archer, S., Birdsey, R., Dahm, C., Heath, L., Hicke, J., Hollinger, D., Huxman, T., Okin, G., Oren, R., Randerson, J., Schlesinger, W., Lettenmaier, D., Major, D., Poff, L., Running, S., Hansen, L., Inouye, D., Kelly, B. P., Meyerson, L, Peterson, B., and Shaw, R.: The Effects of Climate Change on Agriculture, Land Resources, Water Resources, and Biodiversity in the

HESSD
10, 6359–6406, 2013

Integrated assessment of US Midwest water resources

N. Voisin et al.

United States, Chapter, A Report by the US Climate Change Science Program and the Subcommittee on Global Change Research, US Environmental Protection Agency, Washington, DC, USA, 2008.
Biemans, H., Haddeland, I., Kabat, P., Ludwig, F., Hutjes, R. W. A., Heinke, J., von Bloh, W., and Gerten, D.: Impact of reservoirs on river discharge and irrigation water supply during the 20th century, Water Resour. Res., 47, W03509, doi:10.1029/2009WR008929, 2011.
Brenkert, A., Smith S., Kim, S., and Pitcher, H.: Model Documentation for the MiniCAM, PNNL-14337, Pacific Northwest National Laboratory, Richland, Washington, 2003.
Calvin, K., Wise, M., Clarke, L., Edmonds, J., Kyle, P., Luckow, P., and Thomson, A.: Implications of simultaneously mitigating and adapting to climate change: initial experiments using GCAM, Climatic Change, 117, 545–560, doi:10.1007/s10584-012-0650-y, 2013.
Chaturvedi, V., Hejazi, M. I., Edmonds, J., Clarke, L., Kyle, P., Davies, E., Wise, M., and Calvin, K.: Climate Policy Implications for Agricultural Water Demand, PNNL-22356, Pacific Northwest National Laboratory, Richland, Washington, 2013.
Christensen, N. S., Wood, A. W., Voisin, N., Lettenmaier, D. P., and Palmer, R. N.: Effects of climate change on the hydrology and water resources of the Colorado River Basin, Climatic Change, 62, 337–363, 2004.
Clarke, L., Edmonds, J., Jacoby, H., Pitcher, H., Reilly, J., and Richels, R.: CCSP Synthesis and Assessment Product 2.1, Part A: Scenarios of Greenhouse Gas Emissions and Atmospheric Concentrations, US Government Printing Office, Washington DC, 2007a.
Clarke, L., Lurz, J., Wise, M., Edmonds, J., Kim, S., Smith, S., and Pitcher, H.: Model Documentation for the MiniCAM Climate Change Science Program Stabilization Scenarios: CCSP Product 2.1a, PNNL Technical Report, PNNL-16735, Pacific Northwest National Laboratory, Richland, WA, USA, 2007b.
Cuo, L., Beyene, T. K., Voisin, N., Su, F., Lettenmaier, D. P., Alberti, M., and Richey, J. E.: Effects of mid-twenty-first century climate and land cover change on the hydrology of the Puget Sound basin, Washington, Hydrol. Process., 25, 1729–1753, doi:10.1002/hyp.7932, 2011.
Davies, E., Kyle, P., and Edmonds, J.: An integrated assessment of global and regional water demands for electricity generation to 2095, Adv. Water Res., 52, 296–313, 2013.
Delworth, T. L., Broccoli, A. J., Rosati, A., Stouffer, R. J., Balaji, V., Beesley, J. A., Cooke, W. F., Dixon, K. W., Dunne, J. P., Dunne, K. A., Durachta, J. W., Findell, K. L., Ginoux, P., Gnanadesikan, A., Gordon, C. T., Griffies, S. M., Gudgel, R., Harrison, M. J., Held, I. M.,

HESSD
10, 6359–6406, 2013

Integrated assessment of US Midwest water resources

N. Voisin et al.

Hemler, R. S., Horowitz, L. W., Klein, S. A., Knutson, T. R., Kushner, P. J., Langenhorst, A. R., Lee, H.-C., Lin, S.-J., Lu, J., Malyshev, S., Milly, P. C. D., Ramaswamy, V., Russell, J. L., Schwarzkopf, M. D., Shevliakova, E., Sirutis, J. J., Spelman, M. J., Stern, W. F., Winton, M., Wittenberg, A. T., Wyman, B., Zeng, F., and Zhang, R.: GFDL's CM2 global coupled climate models – Part 1: Formulation and simulation characteristics, J. Climate, 19, 643–674, 2006.

Döll, P., Fiedler, K., and Zhang, J.: Global-scale analysis of river flow alterations due to water withdrawals and reservoirs, Hydrol. Earth Syst. Sci., 13, 2413–2432, doi:10.5194/hess-13-2413-2009, 2009.

Haddeland, I., Lettenmaier, D. P., and Skaugen, T.: Effects of irrigation on the water and energy balances of the Colorado and Mekong River basins, J. Hydrol., 324, 210–223, 2006.

Hamlet, A. F., Lee, S. Y., Mickelson, K. E. B., and Elsner, M. M.: Effects of projected climate change on energy supply and demand in the Pacific Northwest and Washington State, Climatic Change, 102, 103–128, doi:10.1007/s10584-010-9857-y, 2010.

Hanasaki, N., Kanae, S., and Oki, T.: A reservoir operation scheme for global river routing models, J. Hydrol., 327, 22–41, doi:10.1016/j.jhydrol.2005.11.011, 2006.

Hanasaki, N., Kanae, S., Oki, T., Masuda, K., Motoya, K., Shirakawa, N., Shen, Y., and Tanaka, K.: An integrated model for the assessment of global water resources – Part 1: Model description and input meteorological forcing, Hydrol. Earth Syst. Sci., 12, 1007–1025, doi:10.5194/hess-12-1007-2008, 2008.

Hanasaki, N., Fujimori, S., Yamamoto, T., Yoshikawa, S., Masaki, Y., Hijioka, Y., Kainuma, M., Kanamori, Y., Masui, T., Takahashi, K., and Kanae, S.: A global water scarcity assessment under shared socio-economic pathways – Part 1: Water use, Hydrol. Earth Syst. Sci. Discuss., 9, 13879–13932, doi:10.5194/hessd-9-13879-2012, 2012a.

Hanasaki, N., Fujimori, S., Yamamoto, T., Yoshikawa, S., Masaki, Y., Hijioka, Y., Kainuma, M., Kanamori, Y., Masui, T., Takahashi, K., and Kanae, S.: A global water scarcity assessment under shared socio-economic pathways – Part 2: Water availability and scarcity, Hydrol. Earth Syst. Sci. Discuss., 9, 13933–13994, doi:10.5194/hessd-9-13933-2012, 2012b.

Hejazi, M. I., Edmonds, J., Clarke, L., Kyle, P., Davies, E., Chaturvedi, V., Wise, M., Patel, P., Eom, J., and Calvin, K.: Integrated assessment of global water scarcity over the 21st century – Part 1: Global water supply and demand under extreme radiative forcing, Hydrol. Earth Syst. Sci. Discuss., 10, 3327–3381, doi:10.5194/hessd-10-3327-2013, 2013a.

Hejazi, M. I., Edmonds, J., Clarke, L., Kyle, P., Davies, E., Chaturvedi, V., Eom, J., Wise, M., Patel, P., and Calvin, K.: Integrated assessment of global water scarcity over the 21st century

– Part 2: Climate change mitigation policies, Hydrol. Earth Syst. Sci. Discuss., 10, 3383–3425, doi:10.5194/hessd-10-3383-2013, 2013b.
Hejazi, M. I., Edmonds, J., Chaturvedi, V., Davies, E., and Eom, J.: Scenarios of global municipal water use demand projections over the 21st century, Hydrolog. Sci. J., 58, 1–20, doi:10.1080/02626667.2013.772301, 2013c.
Held, I. M. and Soden, B. J.: Robust responses of the hydrological cycle to global warming, J. Climate, 19, 5686–5699, 2006.
Huang, M., Hou, Z., Leung, L. R., Ke, Y., Liu, Y., Fang, Z., and Sun, Y.: Uncertainty Analysis of runoff simulations and parameter detectability in the community land model – evidence from MOPEX basins and flux tower sites, J. Hydrometeorol., doi:10.1175/JHM-D-12-0138.1, in press, 2013.
Hidalgo, H. G., Dettinger, M., and Cayan, D.: Downscaling with constructed analogues: Daily precipitation and temperature fields over the United States CEC-500-2007-123, California Energy Commission, PIER Energy-Related Environmental Research, available at: http://www.energy.ca.gov/2007publications/CEC-500-2007-123/CEC-500-2007-123.PDF (last access: 2011), 2008.
Ke, Y., Leung, L. R., Huang, M., Coleman, A. M., Li, H., and Wigmosta, M. S.: Development of high resolution land surface parameters for the Community Land Model, Geosci. Model Dev., 5, 1341–1362, doi:10.5194/gmd-5-1341-2012, 2012.
Kenny, J. F., Barber, N. L., Hutson, S. S., Linsey, K. S., Lovelace, J. K., and Maupin, M. A.: Estimated use of water in the United States in 2005, US Geological Survey Circular 1344, 52, available at: http://water.usgs.gov/watuse/ (last access: February 2011), 2009.
Kim, S. H., Edmonds, J. A., Lurz, J., Smith, S. J., and Wise, M. A.: The object-oriented energy climate technology system (ObjECTS) framework and hybrid modeling of transportation in the MiniCAM long-term, global integrated assessment model, Energ. J., 27, 63–92, doi:10.5547/ISSN0195-6574-EJ-VolSI2006-NoSI2-4, 2006.
Kimball, J. S., Running, S. W., and Nemani, R. R.: An improved method for estimating surface humidity from daily minimum temperature, Agr. Forest Meteorol., 85, 87–98, 1997.
Konar, M., Hussein, Z., Hanasaki, N., Mauzerall, D. L., and Rodriguez-Iturbe, I.: Virtual water trade flows and savings under climate change, Hydrol. Earth Syst. Sci. Discuss., 10, 67–101, doi:10.5194/hessd-10-67-2013, 2013.
Kraucunas, I. P., Clarke, L. E., Dirks, J. A., Hejazi, M. I., Hibbard, K. A., Huang, M., Kintner-Meyer, M. C. W., Kleese van Dam, K., Leung, L. Y. R., Moss, R. H. Peterson, M. J., Rice, J.

S., Scott, M. J., Thomson, A. M., and West, T. O.: Investigating the nexus of climate, energy, water, and land at decision-relevant scales: the Platform for Regional Integrated Modeling and Analysis (PRIMA), Climatic Change, submitted, 2013.

Kyle, P., Davies, E., Dooley, J. J., Smith, S. J., Clarke, L., Edmonds, J., and Hejazi, M. I.: Influence of climate change mitigation technology on global demands of water for electricity generation, Int. J. Greenh. Gas Con., 13, 112–123, doi:10.1016/j.ijggc.2012.12.006, 2013.

Lawrence, D. M., Oleson, K. W. , Flanner, M. G., Thornton, P. E., Swenson, S. C., Lawrence, P. J., Zeng, X., Yang, Z.-L., Levis, S., Sakaguchi, K., Bonan, G. B., and Slater, A. G.: Parameterization improvements and functional and structural advances in version 4 of the Community Land Model, J. Adv. Model. Earth Sys., 3, M03001, doi:10.1029/2011MS000045, 2011

Lehner, B., Liermann, C. R., Revenga, C., Vorosmarty, C., Fekete, B., Crouzet, P., Doll, P., Endejan, M., Frenken, K., Magome, J., Nilsson, C., Robertson, J. C., Rodel, R., Sindorf, N., and Wisser, D.: Global Reservoir and Dam Database, Version 1 (GRanDv1): Reservoirs, Revision 01. Digital Water Atlas at GWSP, available at: http://www.gwsp.org/85.html (last access: 26 September 2011), 2011a.

Lehner, B., Liermann, C. R., Revenga, C., Vörösmarty, C., Fekete, B., Crouzet, P., Döll, P., Endejan, M., Frenken, K., Magome, J., Nilsson, C., Robertson, J. C., Rödel, R., Sindorf, N., and Wisser, D.: High-resolution mapping of the world's reservoirs and dams for sustainable river-flow management, Front. Ecol. Environ., 9, 494–502, doi:10.1890/100125, 2011b.

Leung, L. R., Kuo, Y.-H., and Tribbia, J.: Research needs and directions of regional climate modeling using WRF and CCSM, B. Am. Meteorol. Soc., 87, 1747–1751, 2006.

Li, H., Huang, M., Wigmosta, M., Ke, Y., Coleman, A., Leung, L. R., Wang, A., and Ricciuto, D. M.: Evaluating Runoff Simulations from the Community Land Model 4.0 Using Observations From Flux Towers and a Mountain Watershed, J. Geophys. Res.-Atmos., 116, D24120, doi:10.1029/2011JD016276, 2011.

Li, H., Wigmosta, M. S., Wu, H., Huang, M., Ke, Y., Coleman, A. M., and Leung, L. R.: A physically based runoff routing model for land surface and earth system models, J. Hydrometeorol., doi:10.1175/JHM-D-12-015.1, in press, 2013a.

Li, H.-Y., Huang, M., Tesfa, T., Ke, Y., Sun, Y., Liu, Y., and Leung, L. R.: A subbasin-based framework to represent land surface processes in an Earth System Model, Geosci. Model Dev. Discuss., 6, 2699–2730, doi:10.5194/gmdd-6-2699-2013, 2013b.

HESSD
10, 6359–6406, 2013

Liang, X., Lettenmaier, D. P., Wood, E. F., and Burges, S. J.: A simple hydrologically based model of land surface water and energy fluxes for GSMs, J. Geophys. Res., 99, 14415–14428, 1994.

Mao, D. and Cherkauer, K. A.: Impacts of land-use change on hydrologic responses in the Great Lakes region, J. Hydrol., 374, 71–82, 2009.

Maurer, E. P. and Lettenmaier, D. P.: Predictability of seasonal runoff in the Mississippi River basin, J. Geophys. Res., 108, 8607, doi:10.1029/2002JD002555, 2003.

Maurer, E. P., Wood, A. W., Adam, J. C., Lettenmaier, D. P., and Nijssen, B.: A long-term hydrologically-based data set of land surface fluxes and states for the conterminous United States, J. Climate, 15, 3237–3251 , 2002.

Maurer, E. P., Hidalgo, H. G., Das, T., Dettinger, M. D., and Cayan, D. R.: The utility of daily large-scale climate data in the assessment of climate change impacts on daily streamflow in California, Hydrol. Earth Syst. Sci., 14, 1125–1138, doi:10.5194/hess-14-1125-2010, 2010.

Mishra, M., Cherkauer, K. A., Niyogi, D., Lei, M., Pijanowski, B. C., Ray, D. K., Bowling, L. C., and Yang, G.: A regional scale assessment of land use/land cover and climatic changes on water and energy cycle in the upper Midwest United States, Int. J. Climatol., 30, 2025–2044, doi:10.1002/joc.2095, 2010.

Monfreda, C., Ramankutty, N., and Hertel, T.: Global agricultural land use data for climate change analysis, in: Economic Analysis of Land Use in Global Climate Change Policy, edited by: Hertel, T., Rose, S., and Tol, R., Routledge, New York, 368 pp., 2009.

Pokhrel, Y., Hanasaki, N., Koirala, S., Cho, J., Yeh, P. J.-F., Kim, H., Kanae, S., and Oki, T.: Incorporating Anthropogenic Water Regulation Modules into a Land Surface Model, J. Hydrometeor., 13, 255–269, doi:10.1175/JHM-D-11-013.1, 2012.

Siebert, S. and Döll, P.: The Global Crop Water Model (GCWM): documentation and first results for irrigated crops, Frankfurt Hydrology Paper 07, Institute of Physical Geography, University of Frankfurt, Frankfurt am Main, Germany, 2008.

Sivapalan, M., Savenije, H., and Bloschl, G.: Socio-hydrology: a new science of people and water, Hydrol. Process., 26, 1270–1276, 2012.

Tamea, S., Allamano, P., Carr, J. A., Claps, P., Laio, F., and Ridolfi, L.: Local and global perspectives on the virtual water trade, Hydrol. Earth Syst. Sci., 17, 1205–1215, doi:10.5194/hess-17-1205-2013, 2013.

HESSD

10, 6359–6406, 2013

Thornton, P. E. and Running, S. W.: An improved algorithm for estimating incident daily solar radiation from measurements of temperature, humidity, and precipitation, Agr. Forest Meteorol., 93, 211–228, 1999.
Thornton, P. E., Hasenauer, H., and White, M. A.: Simultaneous estimation of daily solar radiation and humidity from observed temperature and precipitation: an application over complex terrain in Austria, Agr. Forest Meteorol., 104, 255–271, doi:10.1016/S0168-1923(00)00170-2, 2000.
TVA (Tennessee Valley Authority): Heat and Mass Transfer Between a Water Surface and the Atmosphere, Engineering Laboratory Report No. 14, Norris, TN, USA, 1972.
Vano, J. A., Voisin, N., Cuo, L., Hamlet, A. F., Elsner, M. M., Palmer, R. N., Polebitski, A., and Lettenmaier, D. P.: Climate change impacts on water management in the Puget Sound region, Washington, USA, Climatic Change, 102, 225–260, doi:10.1007/s10584-010-9846-1, 2010.
Vano, J. A., Scott, M., Voisin, N., Stöckle, C. O., Hamlet, A. F., Mickleson, K. E. B., Elsner, M. M., and Lettenmaier, D. P.: Climate change impacts on water management and irrigated agriculture in the Yakima River basin, Washington, USA, Climatic Change, 102, 287–317, doi:10.1007/s10584-010-9856-z, 2010.
Van Rheenen, N. T., Wood, A. W., Palmer, R. N., and Lettenmaier, D. P.: Potential implications of PCM climate change scenarios for Sacramento – San Joaquin River Basin Hydrology and Water Resources, Climatic Change, 62, 257–281, 2004.
Voisin, N., Li, H., Ward, D., Huang, M., Wigmosta, M., and Leung, L. R.: On an improved sub-regional water resources management representation for integration into earth system models, Hydrol. Earth Syst. Sci. Discuss., 10, 3501–3540, doi:10.5194/hessd-10-3501-2013, 2013.
Wada, Y., van Beek, L. P. H., Viviroli, D., Dürr, H. H., Weingartner, R., and Bierkens, M. F. P.: Global monthly water stress: 2. Water demand and severity of water stress, Water Resour. Res., 47, W07518, doi:10.1029/2010WR009792, 2011.
Wise, M., Calvin, K., Thomson, A., Clarke, L., Bond-Lamberty, B., Sands, R., Smith, S. J., Janetos, A., and Edmonds, J.: Implications of limiting CO_2 concentrations for land use and energy, Science, 324, 1183–1186, 2009.
Yuan, H., Dai, Y., Xiao, Z., Ji, D., and Wang, S.: Reprocessing the MODIS leaf area index products for land surface and climate modeling, Remote Sens. Environ., 115, 1171–1187, 2011.

HESSD
10, 6359–6406, 2013

Integrated assessment of US Midwest water resources

N. Voisin et al.

HESSD
10, 6359–6406, 2013

Integrated assessment of US Midwest water resources

N. Voisin et al.

Table 1. Correlation coefficients between GCAM and USGS based on state-level water demand estimates by sector; correlation values in parenthesis are based on the Miwestern states only.

Water demand sectors	1990 Consumption	1990 Withdrawal	2005 Withdrawal*
Irrigation	0.86 (0.80)	0.75 (0.91)	0.77 (0.99)
Non-irrigation	0.78 (0.77)	0.58 (0.93)	0.80 (0.87)
Total	0.84 (0.80)	0.77 (0.57)	0.87 (0.87)

* USGS does not provide consumptive water use data for 2005.

Table 2. Percent change in annual discharge of the simulated regulated flow with respect to the simulated natural discharge.

Period	Midwest	Missouri	Ohio	Upper Mississippi
Hist.	−7.9 %	−24.2 %	−0.8 %	−6.6 %
2030s	−11.1 %	−31.6 %	−2.2 %	−10.8 %
2050s	−13.7 %	−36.9 %	−2.4 %	−12.7 %
2080s	−12.0 %	−34.1 %	−1.6 %	−11.2 %

HESSD
10, 6359–6406, 2013

Table 3. Total annual supply deficit as a percent of total annual water demand.

Period	Midwest	Missouri	Ohio	Upper Mississippi
Hist.	3.1 %	1.5 %	3.5 %	8.2 %
2030s	7.2 %	5.4 %	5.7 %	13.2 %
2050s	9.1 %	7.6 %	6.1 %	14.8 %
2080s	9.7 %	9.0 %	6.2 %	13.3 %

HESSD
10, 6359–6406, 2013

Table 4. Fraction of total demand attributed to the irrigation sector.

Period	Midwest	Missouri	Ohio	Upper Mississippi
Hist.	0.8	0.9	0.35	0.75
2030s	0.82	0.9	0.44	0.8
2050s	0.84	0.92	0.47	0.81
2080s	0.85	0.93	0.42	0.71

HESSD
10, 6359–6406, 2013

Table 5. Water balance comparison of GFDL against NLDAS (P = precipitation; R = total runoff; ET = Evapotranspiration) for the Upper Midwest region.

	GFDL		NLDAS	
	1984–1999	1976–1999	1984–1999	1979–2008
P	688	693	712	712
R	157	162	198	195
ET	525	531	516	516
R+ ET	683	693	714	712
P – (R+ ET)	5.1	0.4	–2.5	0.7

HESSD
10, 6359–6406, 2013

HESSD
10, 6359–6406, 2013

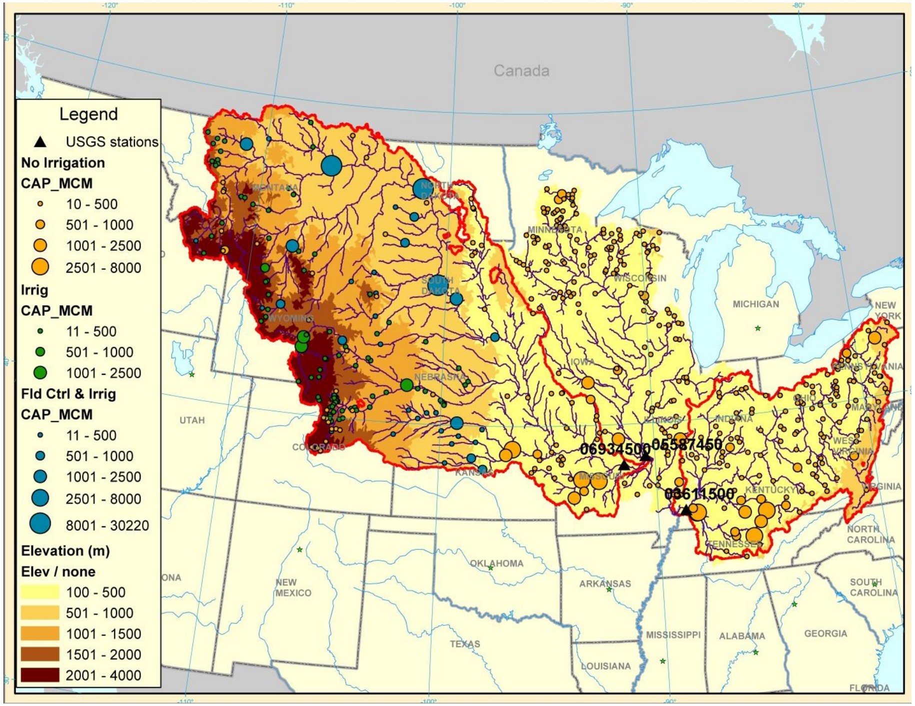

Fig. 1. GRanD reservoir database by type of operating rules over the three regions of the Midwest: Missouri, Upper Mississippi and Ohio. Flow is validated at the outlet of the three regions: Missouri at Hermann (06934500), Upper Mississippi at Grafton (05587450) and Ohio at Metropolis (03611500).

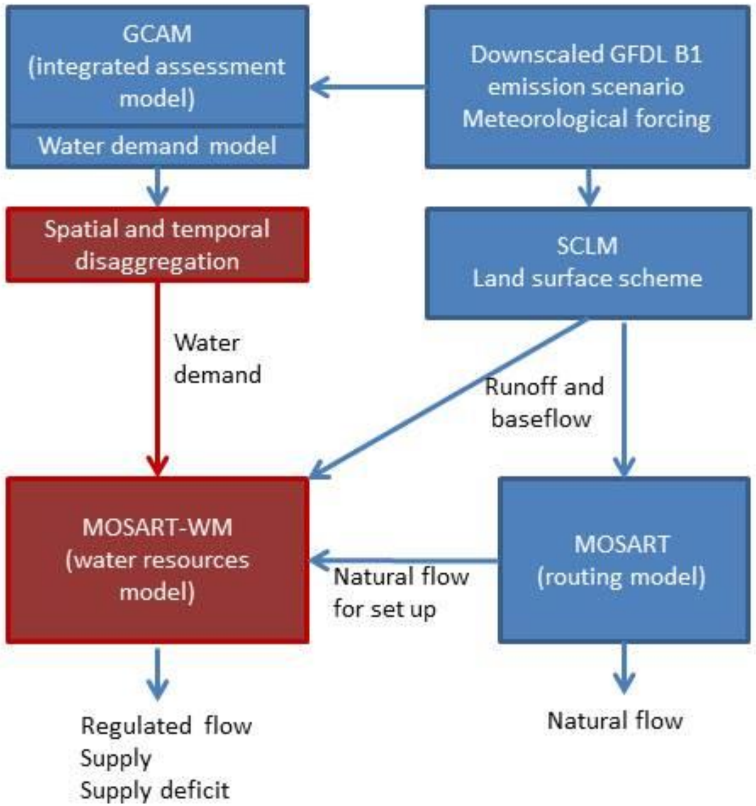

Fig. 2. Schematic of the system. The paper describes and evaluates the coupling of the water demand model with the water resources model (red).

HESSD
10, 6359–6406, 2013

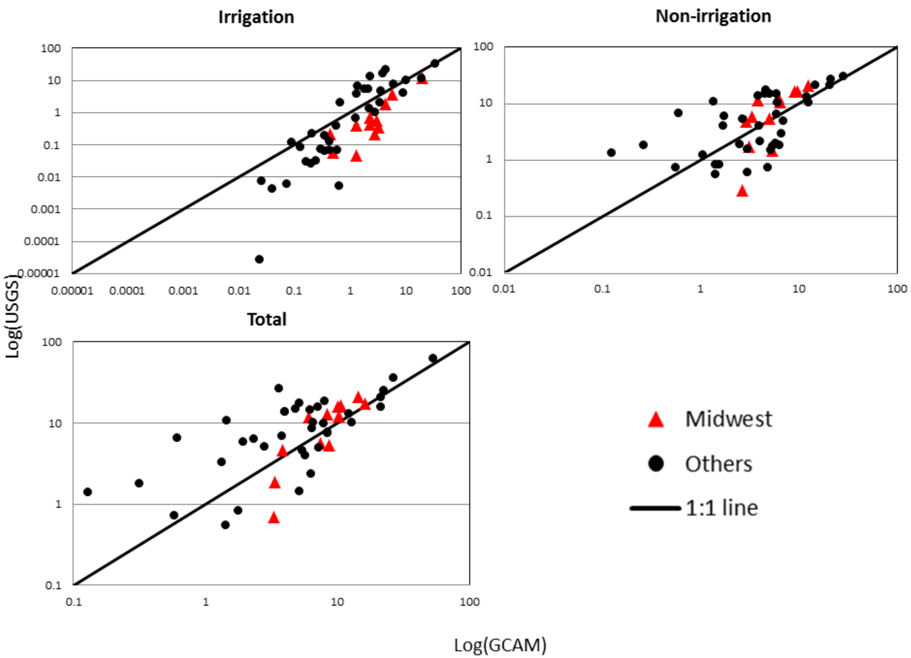

Fig. 3. Comparison of GCAM water withdrawal values in year 2005 to USGS values (log-log scale) by states of the United States, and for the Midwestern states.

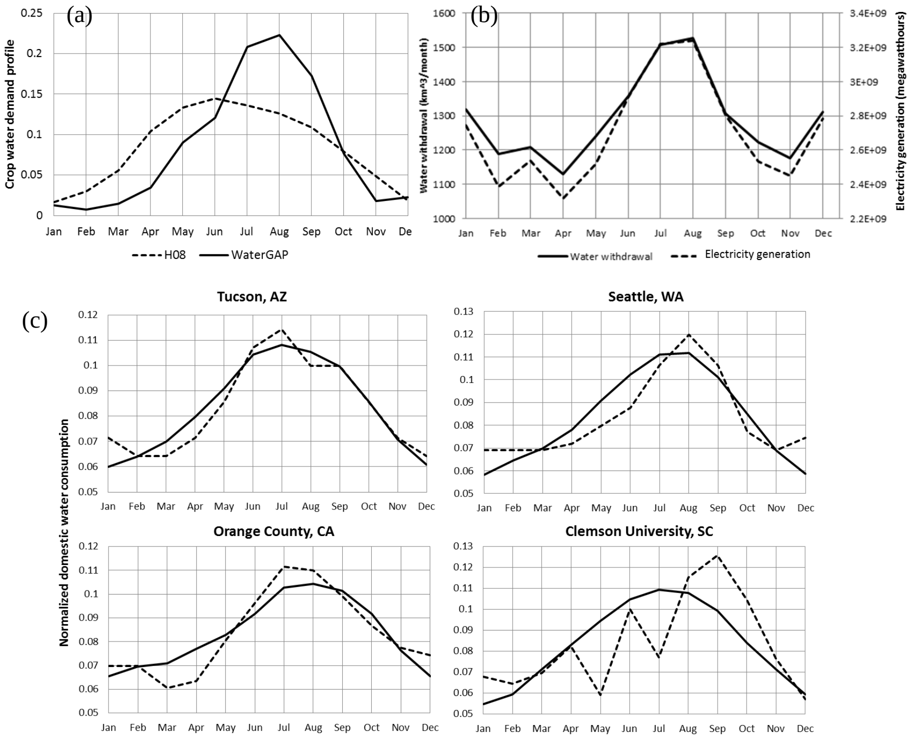

Fig. 4. Temporally downscaling GCAM's annual water demands to monthly profiles: **(a)** irrigation water demand profiles averaged over all AEZs from two models; **(b)** US monthly water withdrawal for electricity generation for the year 2005; **(c)** normalized monthly domestic water consumption for Tucson, AZ, Seattle, WA, Orange County, CA and Clemson University, SC; the dashed line is calculated based on reported water consumption and the solid line is calculated from 1990 GCAM output using Eq. (7).

HESSD
10, 6359–6406, 2013

Integrated assessment of US Midwest water resources

N. Voisin et al.

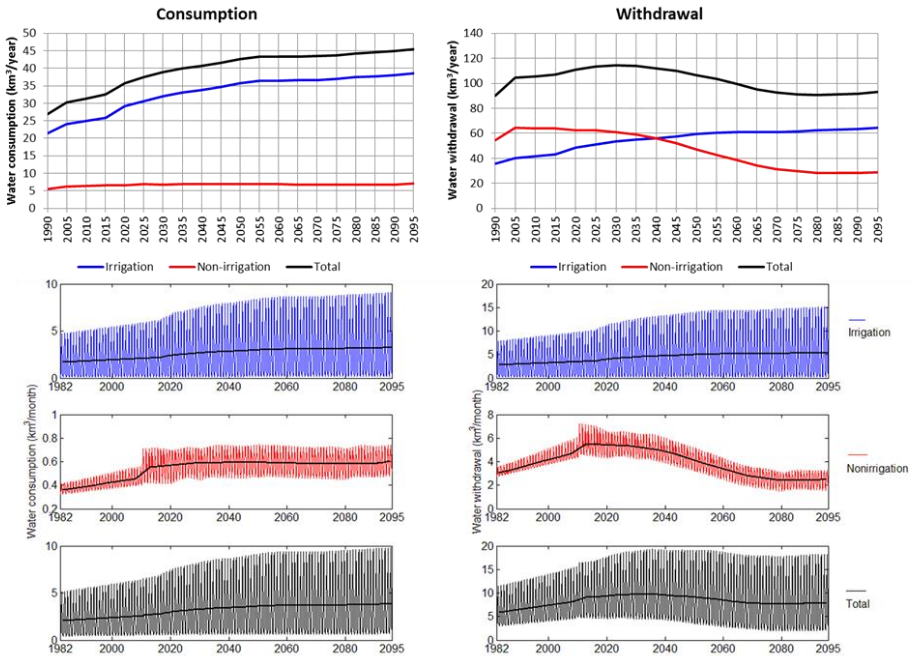

Fig. 5. (a) Annual water demand by sector from GCAM for the time period of 1990–2095 under B1 scenario. **(b)** Monthly downscaled water demand by sector for the time period of 1982–2095 under B1 scenario.

HESSD
10, 6359–6406, 2013

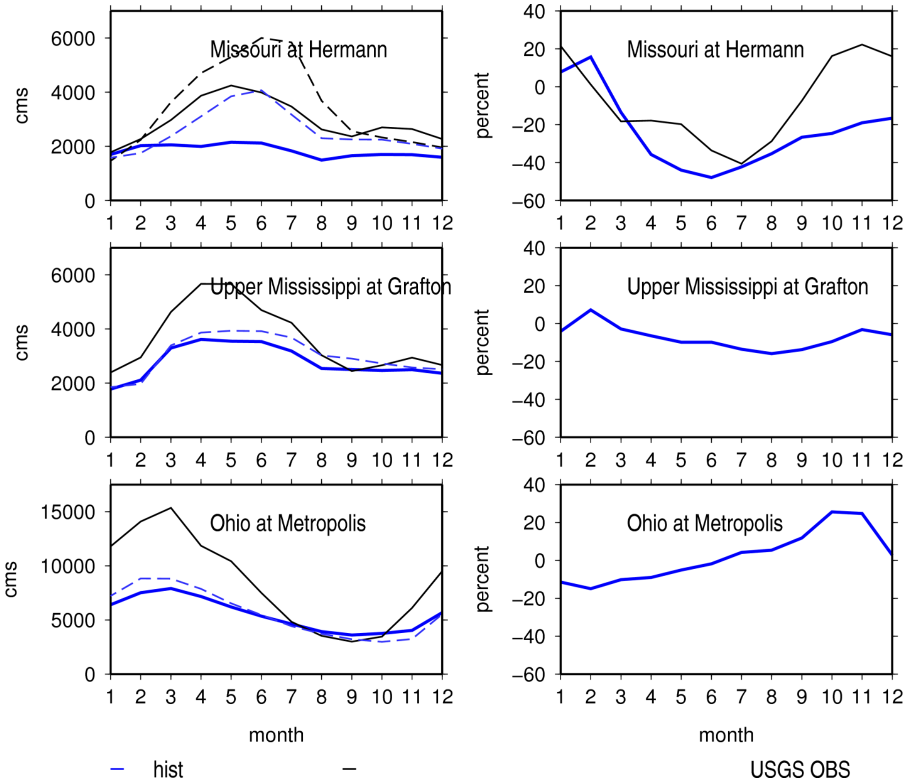

Fig. 6. Simulated natural (dashed) and regulated (solid) flow (left column) and relative change in flow due to regulation (right column) over the three Midwestern regions: Missouri, Upper Mississippi and Ohio for the historical (1984–1999).

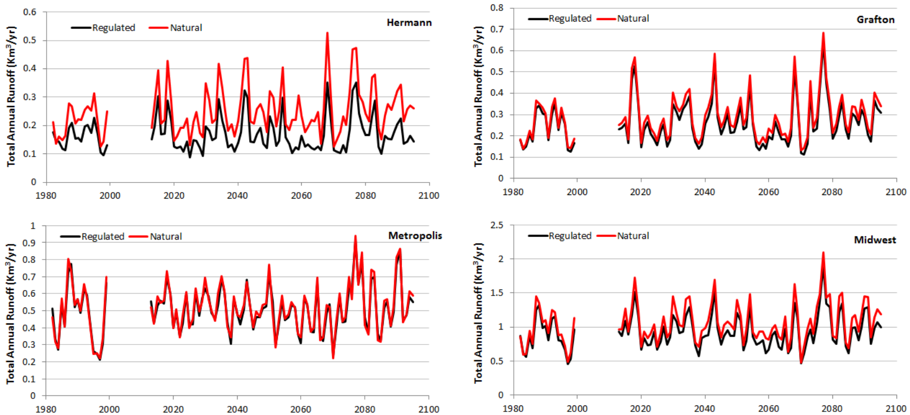

Fig. 7. Long term simulated time series of historical and future (B1) total annual regulated and natural runoff for the three regions and the Upper Midwest.

HESSD
10, 6359–6406, 2013

Integrated assessment of US Midwest water resources

N. Voisin et al.

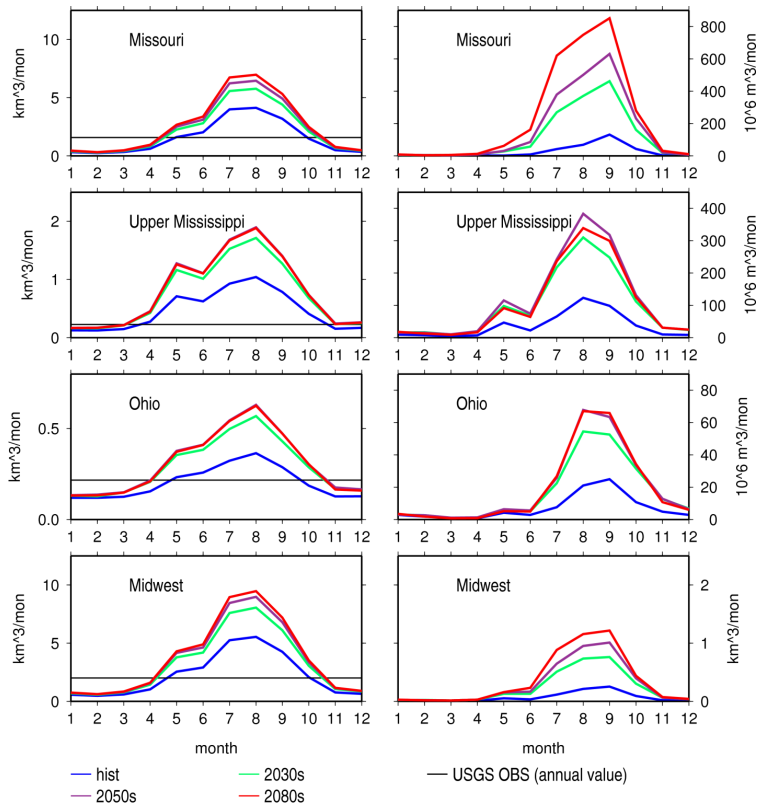

Fig. 8. Monthly average of total water demand (left), and supply deficit (right) over the three regions and over the entire domain for different time periods.

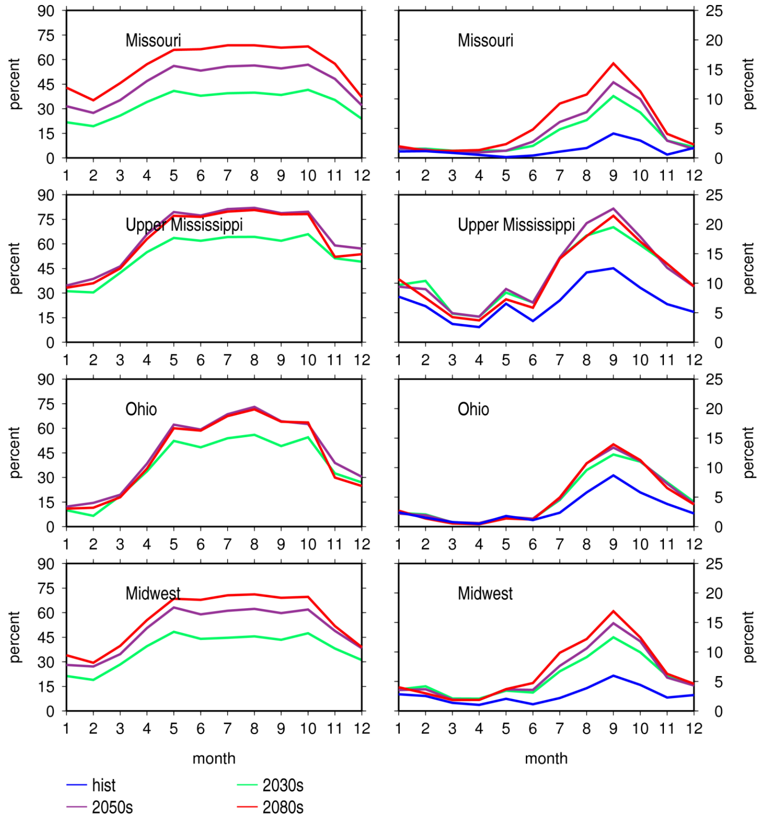

Fig. 9. Relative change in total GCAM demand with respect to the historical demand for the three regions (left), and regional mean monthly fractional water supply deficit – or reliance on another water supply – for historical and future periods.

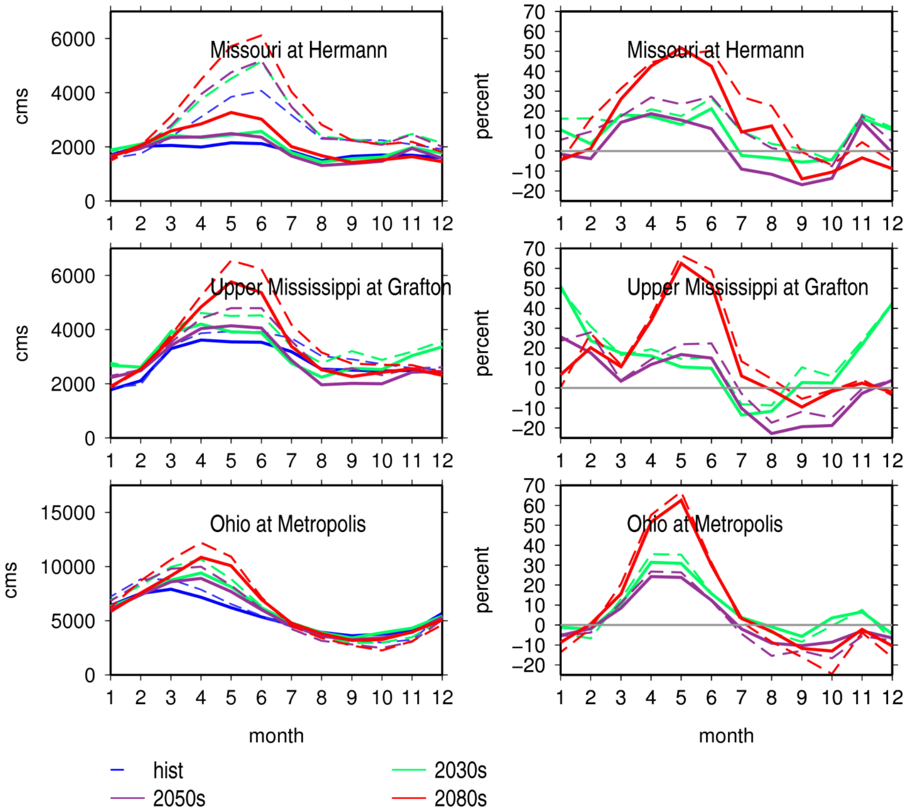

Fig. 10. Left column: simulated mean monthly natural (dashed) and regulated (solid) flow at Hermann, Grafton and Metropolis for different time period: historical (1998–1999), 2030s (2015–45), 2050s (2035–2065) and 2080s (2065–2095). Right column: relative change in duplicate mean monthly flow of natural (dashed) and regulated (solid) flow for future periods with respect to their historical counterparts.

HESSD
10, 6359–6406, 2013

Integrated assessment of US Midwest water resources

N. Voisin et al.

Title Page
Abstract Introduction
Conclusions References
Tables Figures
◀| |▶
◀ ▶
Back Close
Full Screen / Esc
Printer-friendly Version
Interactive Discussion

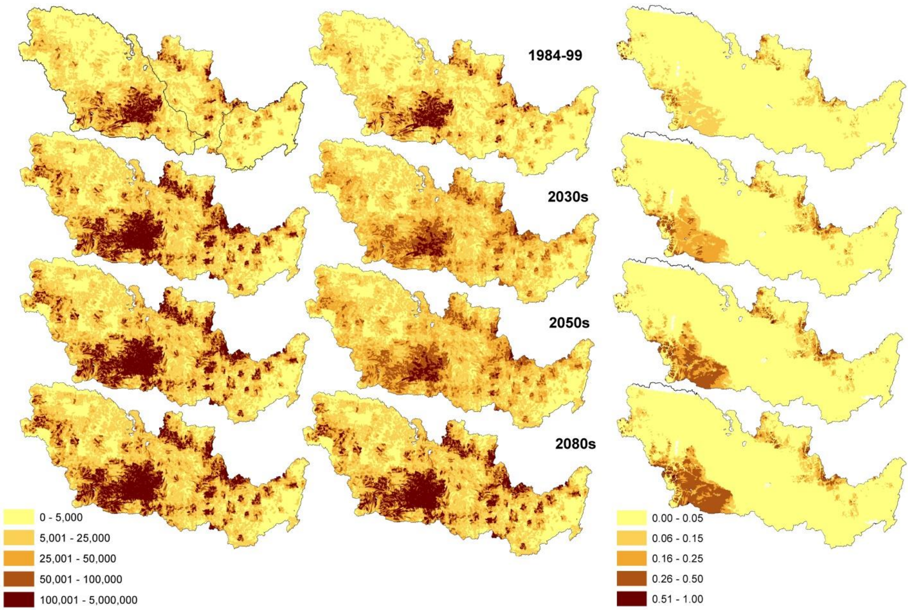

Fig. 11. Annual total water demand (left) and water supply (center) in cubic meters, and fractional water supply deficit for historical and future periods.

HESSD
10, 6359–6406, 2013

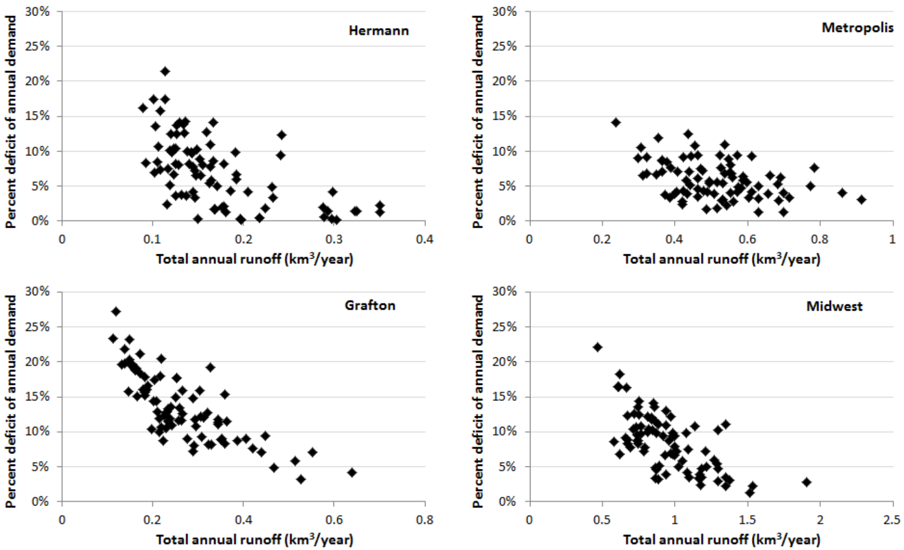

Fig. 12. Relationship between total annual regulated runoff and percent deficit of annual water demand for the historical and future simulations, over the three regions and the Upper Midwest.

HESSD
10, 6359–6406, 2013

Integrated assessment of US Midwest water resources

N. Voisin et al.